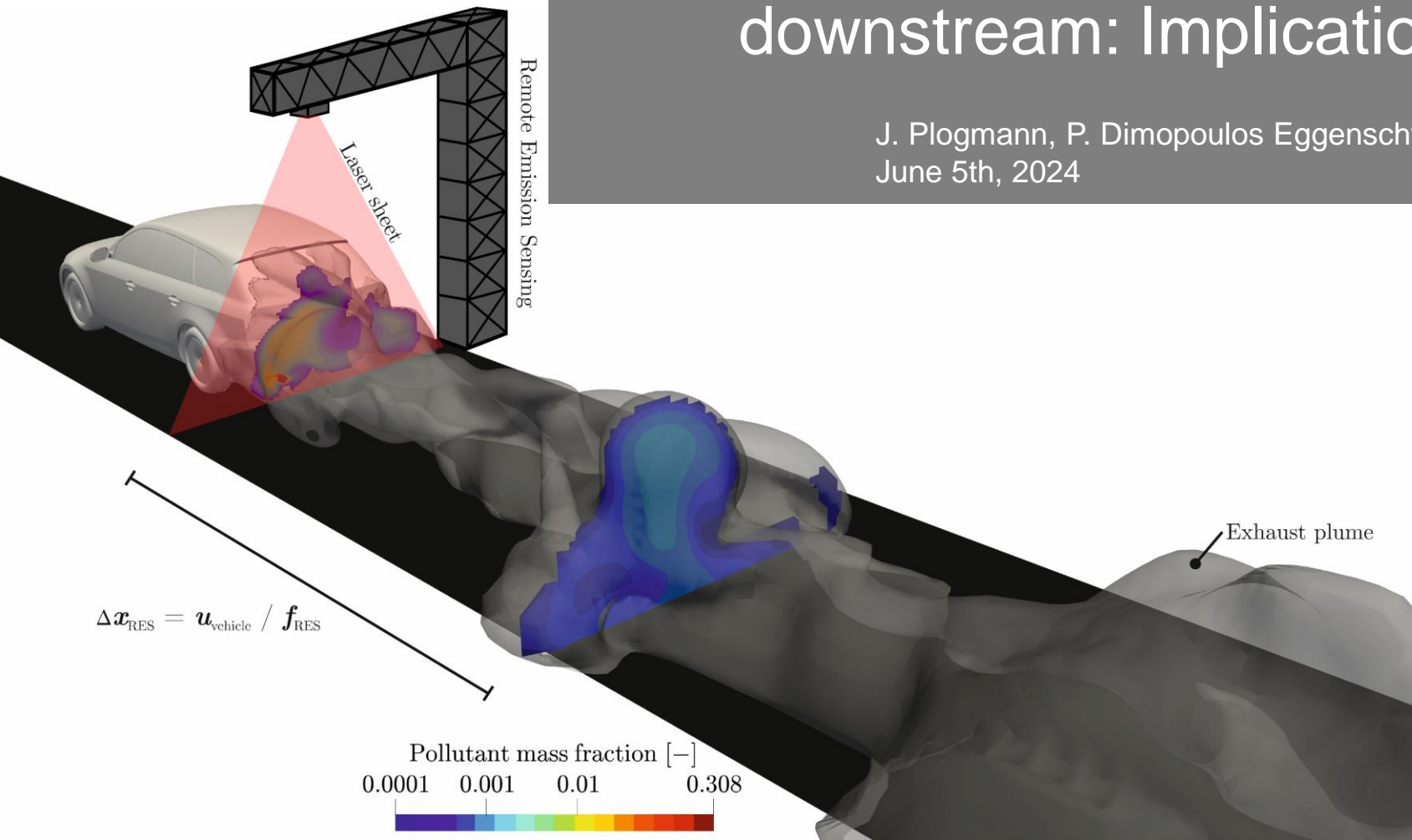
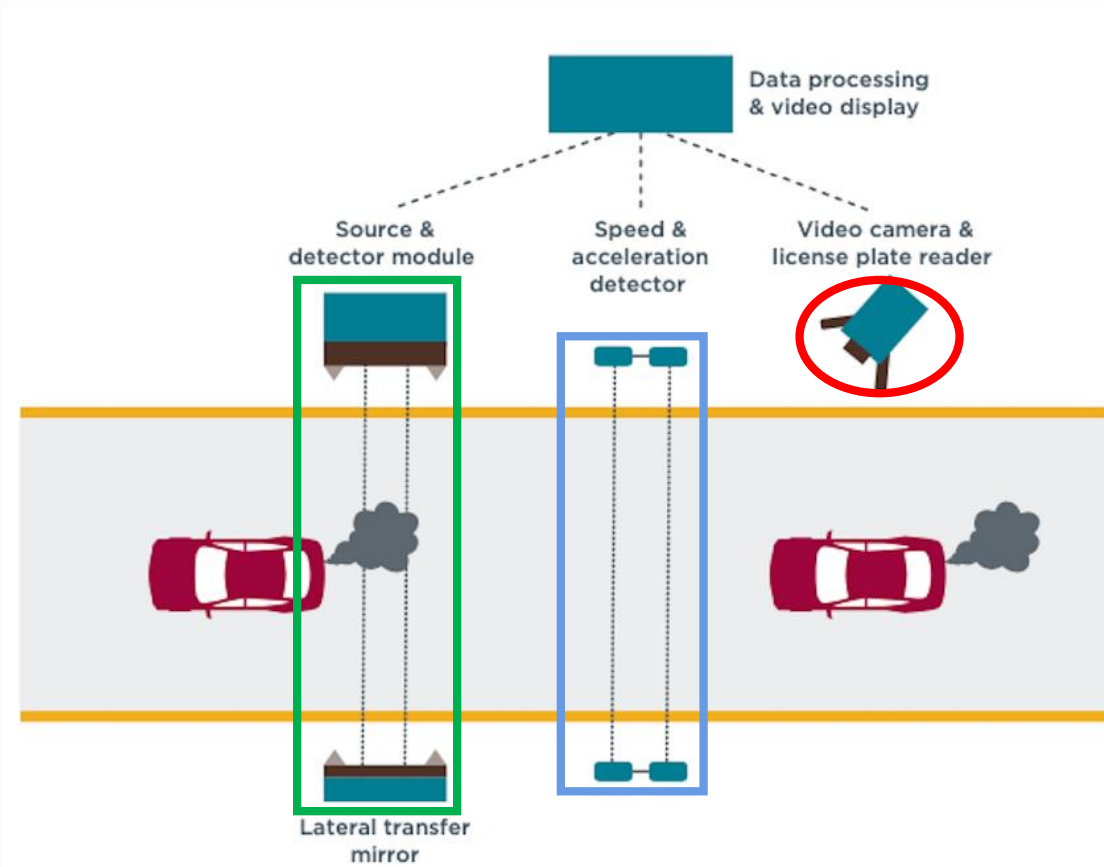


Numerical Simulation of the flow in the vehicle downstream: Implications for Remote Sensing

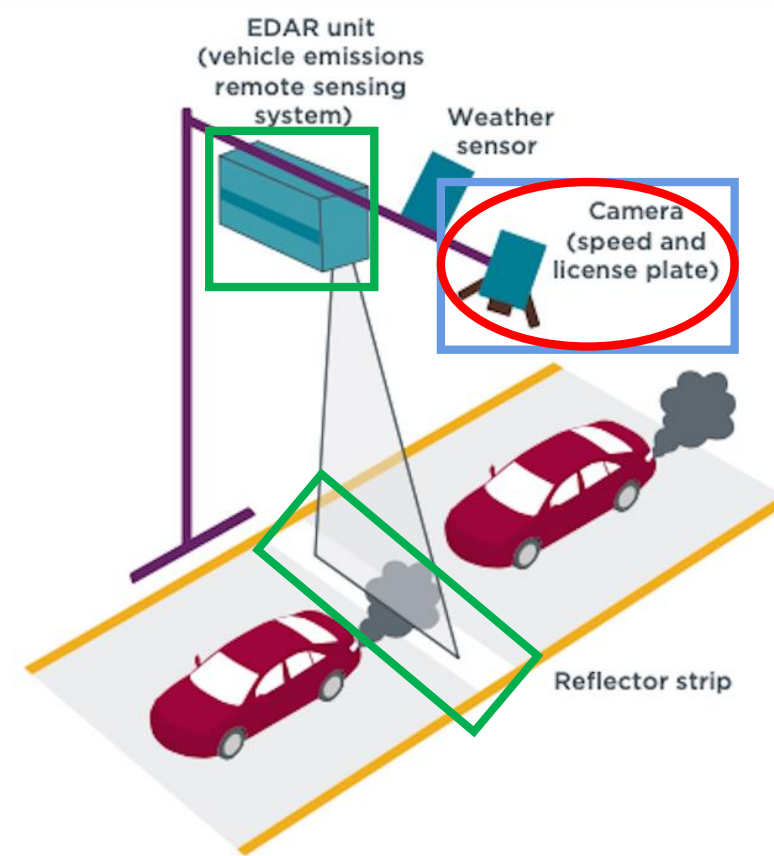
J. Plogmann, P. Dimopoulos Eggenschwiler
June 5th, 2024



There are two types of RES systems available



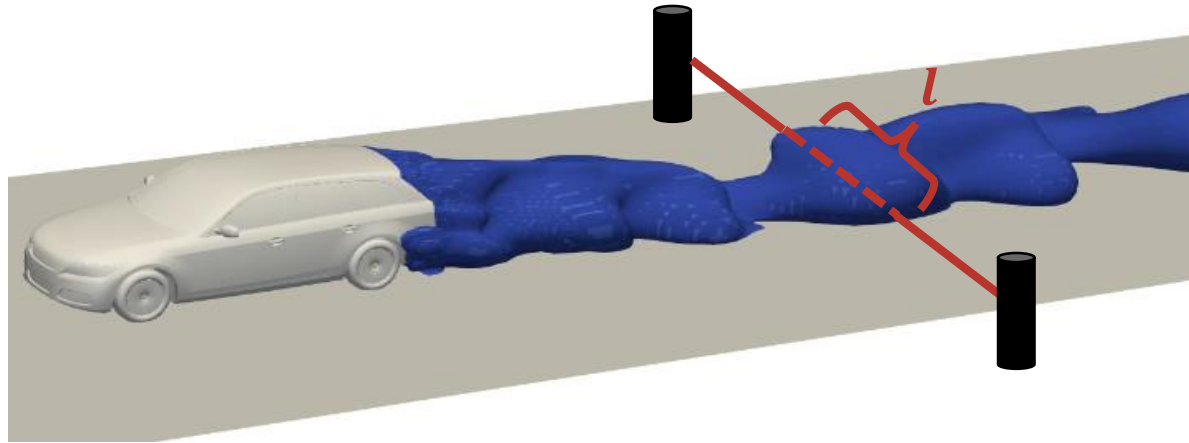
FEAT : Fuel Efficient Automobile Test



EDAR : Emission Detector And Reporting

Source: Anenberg, S., Miller, J., Minjares, R. *et al.* Impacts and mitigation of excess diesel-related NO_x emissions in 11 major vehicle markets. *Nature* **545**, 467–471 (2017).
<https://doi.org/10.1038/nature22086>

The result of a RES measurement is in gr pollutant per gr CO₂



Normal substances: CO₂, H₂O, N₂, O₂
Pollutants: CO, NO, NO₂, C₂H₄ (THC)

Simulation of the exhaust plume

What is measured by the remote sensor: $\frac{\text{Pollutants}}{\text{Fuel consumption}} \propto \frac{c_{\text{NO}_x}}{c_{\text{CO}_2}}$

Relation calibrated in laboratory: Voltage $\propto \frac{1}{A_\lambda}$

Beer-Lambert law:

$$A_\lambda = \epsilon_\lambda \cdot c \cdot l$$

$$c = \frac{A_\lambda}{\epsilon_\lambda \cdot l}$$

- A Optical attenuation
- ϵ Molar attenuation coefficient (adsorptivity)
- c Concentration of species
- l Optical path length

Focus: Simulations and specific evaluations of measurement data



- WP 1: Numerical Simulation of the dispersion of a pollutant in the vehicle
- WP2: Relation of RES measured data to the actual vehicle emission
- WP 3: Potential of RES measurements for determining aging of vehicles' exhaust aftertreatment systems in the field
- WP 4: Technical exchange with the other countries in the project, other projects. Integration of the Swiss measurements in the CONOx database

Focus: Simulations and specific evaluations of measurement data



- WP 1: **Numerical Simulation of the dispersion of a pollutant in the vehicle**
- WP2: Relation of RES measured data to the actual vehicle emission
- WP 3: Potential of RES measurements for determining aging of vehicles' exhaust aftertreatment systems in the field
- WP 4: Technical exchange with the other countries in the project, other projects. Integration of the Swiss measurements in the CONOx database

Flow in the vehicle wake: unsteady, turbulent, heat and species transport



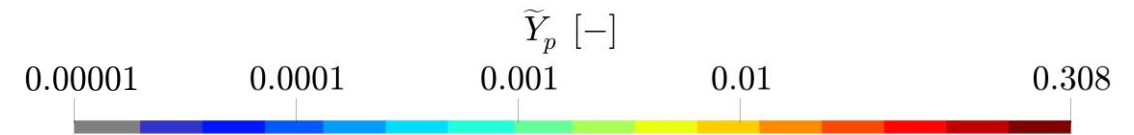
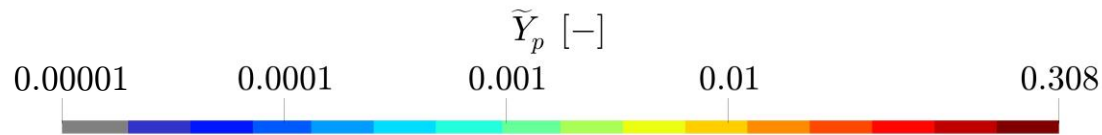
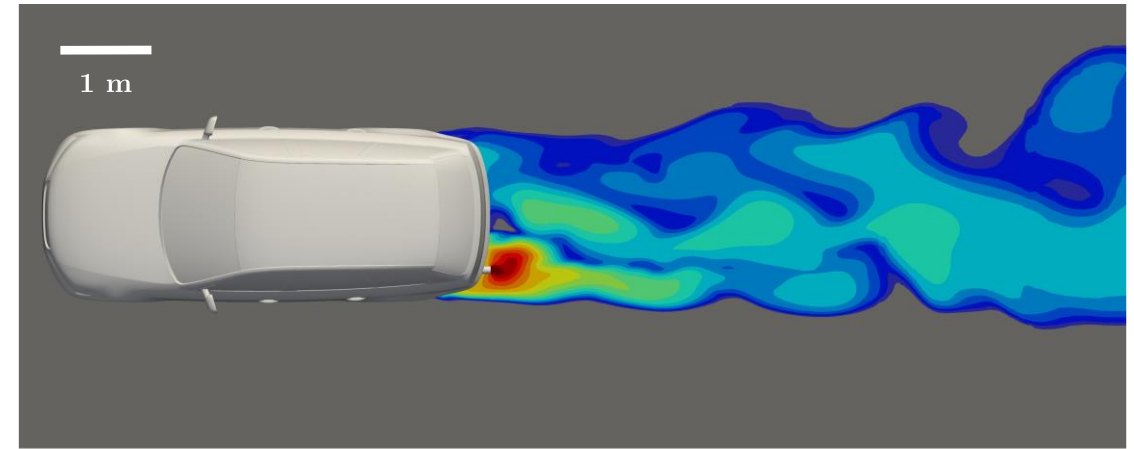
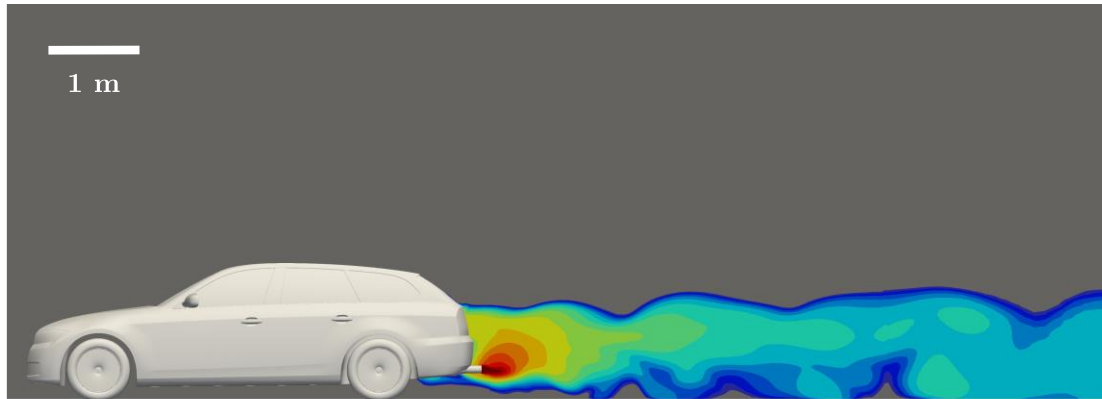
URANS

$$v_{\text{vehicle}} = 50 \text{ km/h}$$

$$Re_L = 4,257,166$$



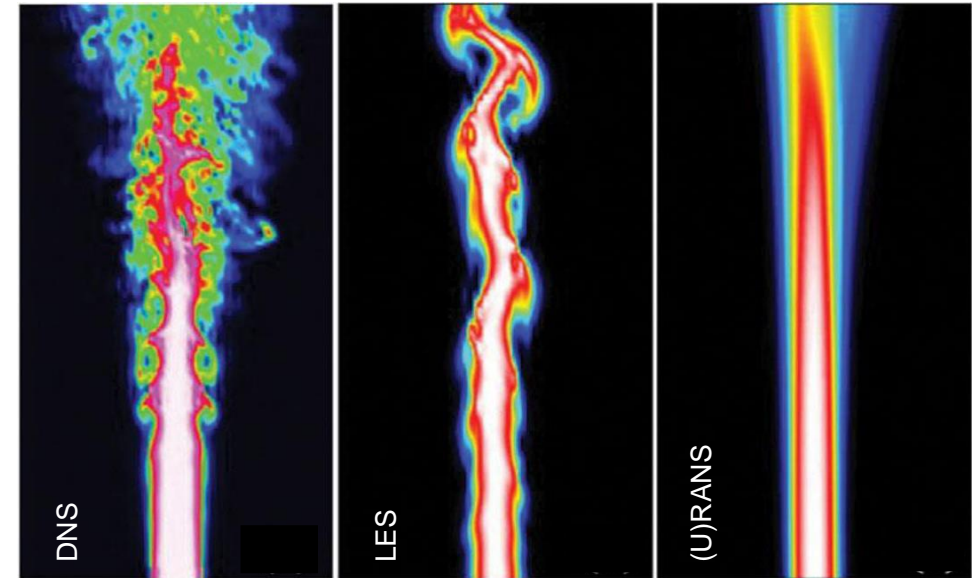
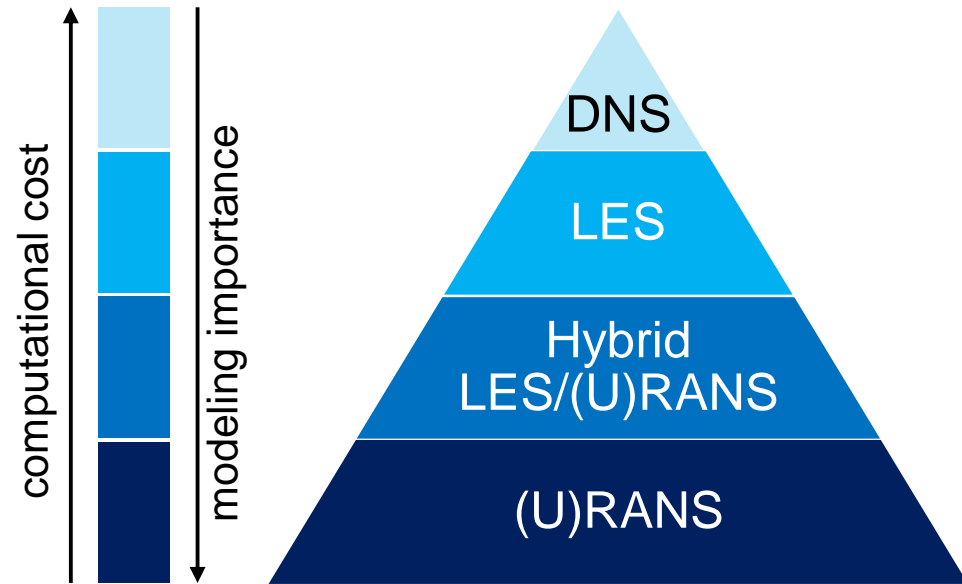
Pollutant concentrations decay rapidly in the vehicle wake



Source: Plogmann, J.; Stauffer, C.; Dimopoulos Eggenschwiler, P.; Jenny, P. URANS Simulations of Vehicle Exhaust Plumes with Insight on Remote Emission Sensing. *Atmosphere* **2023**, *14*, 558. <https://doi.org/10.3390/atmos14030558>

- Turbulent dispersion is dominant: $D_{\text{eff}} = D + D_t$ with $D_t \gg D$
- Thus, the modeling of D_t plays a crucial role for an accurate prediction of the plume dispersion

Turbulence is nowadays one of the most important unsolved problems in physics



- The computational cost of DNS and LES is dependent on the Reynolds number: $Re = (u_\infty L)/\nu$
 - DNS scales with Re^3
 - LES scales with $Re^{1.8}$ near the wall and $Re^{0.4}$ in the free-shear region
- (U)RANS only provides information about averaged quantities but at low computational cost



N.S.F. equations \rightarrow Ensemble-Averaging $\tilde{\phi} = \frac{\overline{\rho\phi}}{\bar{\rho}} \rightarrow k-\omega$ SST model

PISO Algorithm
Finite Volume Method

Momentum equation:

$$\frac{\partial(\bar{\rho}\tilde{u}_i)}{\partial t} + \frac{\partial(\bar{\rho}\tilde{u}_i\tilde{u}_j)}{\partial x_j} = -\frac{\partial(\bar{p} + \frac{2}{3}\bar{\rho}k)}{\partial x_i} + \frac{\partial}{\partial x_j} \left[\mu_{\text{eff}} \left(\frac{\partial\tilde{u}_i}{\partial x_j} + \frac{\partial\tilde{u}_j}{\partial x_i} - \frac{2}{3} \frac{\partial\tilde{u}_k}{\partial x_k} \delta_{ij} \right) \right] + \bar{\rho}\tilde{g}_i$$

Total energy equation:

$$\frac{\partial}{\partial t} \left[\bar{\rho} \left(\tilde{e} + \frac{1}{2} \tilde{u}_i \tilde{u}_i + K \right) \right] + \frac{\partial}{\partial x_j} \left[\bar{\rho} \tilde{u}_j \left(\tilde{h} + \frac{1}{2} \tilde{u}_i \tilde{u}_i + K \right) \right] = \frac{\partial}{\partial x_j} \left(\alpha_{\text{eff}} \frac{\partial\tilde{h}}{\partial x_j} \right) + \bar{\rho}\tilde{g}_i\tilde{u}_i$$

Species equation:

$$\frac{\partial(\bar{\rho}\tilde{Y}_k)}{\partial t} + \frac{\partial}{\partial x_i} (\bar{\rho}\tilde{u}_i\tilde{Y}_k) = \frac{\partial}{\partial x_i} \left(\bar{\rho} D_{\text{eff}} \frac{\partial\tilde{Y}_k}{\partial x_i} \right)$$

Equation of state (ideal gas):

$$\bar{p} = \bar{\rho} R \tilde{T} \sum_k^n \frac{\tilde{Y}_k}{W_k}$$

Sutherland law:

$$\mu = \frac{A_s \sqrt{\tilde{T}}}{1 + T_s/\tilde{T}}$$

Schmidt law:

$$Sc = \frac{\mu}{\bar{\rho} D} = 1$$

Prandtl law:

$$Pr = \frac{\mu}{\bar{\rho} \alpha} = 0.9$$

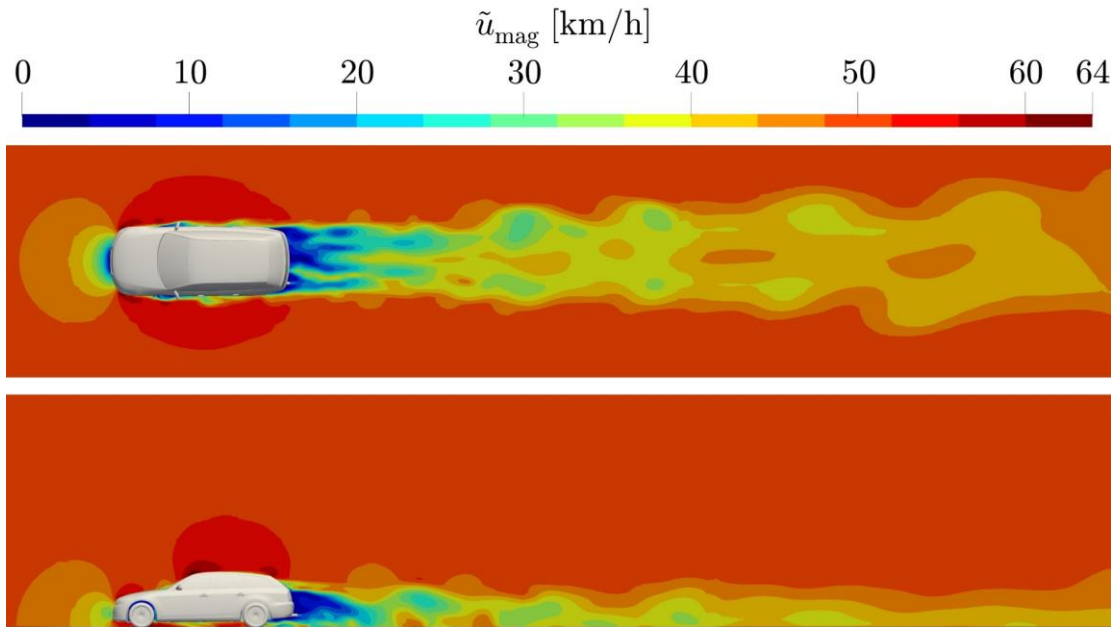
JANAF tables:

c_p, c_v

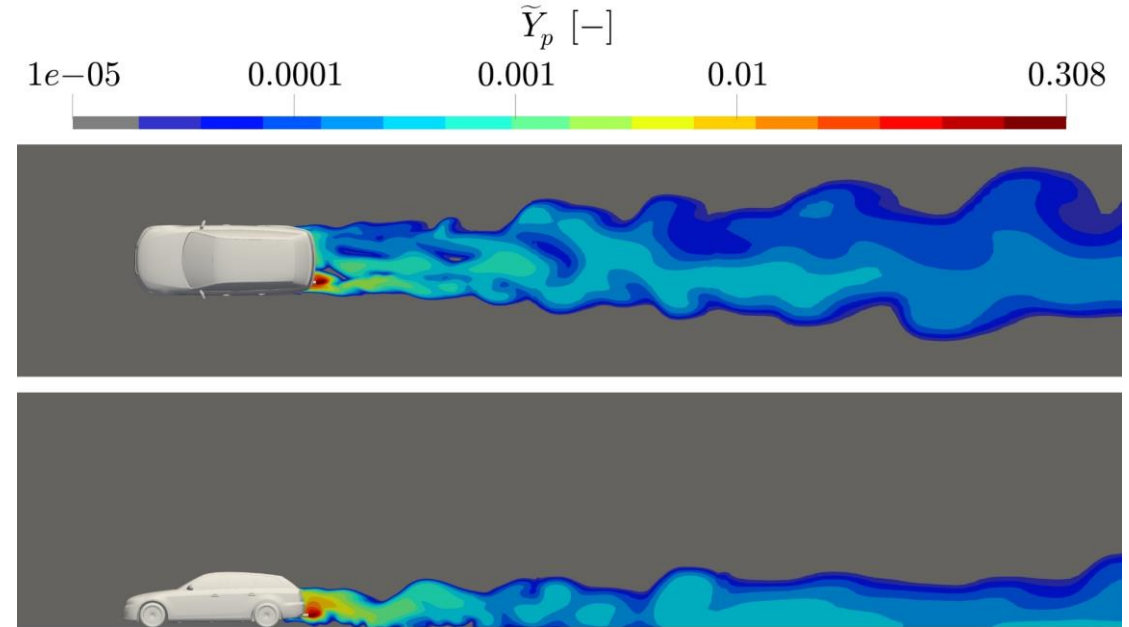
$$Sc_t = \frac{\mu_t}{\bar{\rho} D_t} = 0.7$$

$$Pr_t = \frac{\mu_t}{\bar{\rho} \alpha_t} = 0.9$$

Unsteady and turbulent flow yields time-dependent velocity and pollutant fields

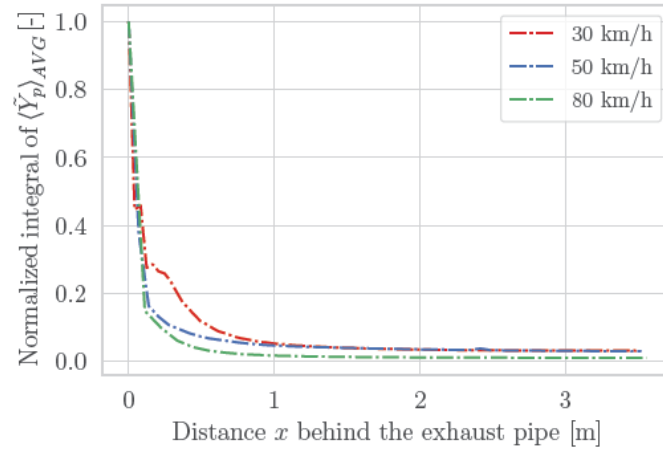


Instantaneous velocity magnitude at $z = 0.3$ m plane (top) and $y = -0.56$ m plane (bottom).

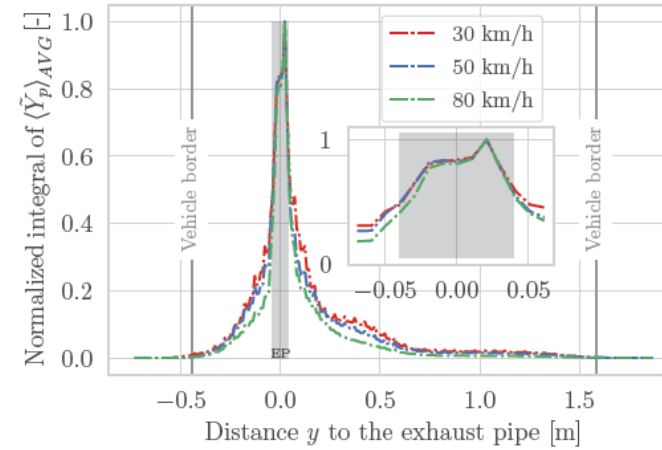


Instantaneous pollutant mass fraction at $z = 0.3$ m plane (top) and $y = -0.56$ m plane (bottom).

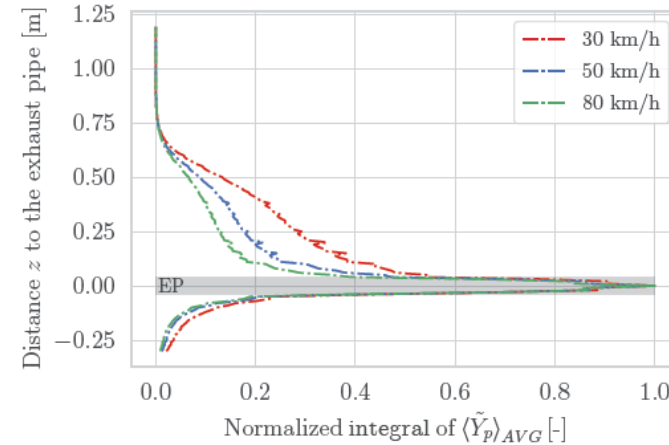
Vehicle speed influences the exhaust plume dispersion in all directions



(a) Normalized cut plane integral of time-averaged pollutant mass fraction in the yz -planes.



(b) Normalized cut plane integral of time-averaged pollutant mass fraction in the xz -planes.

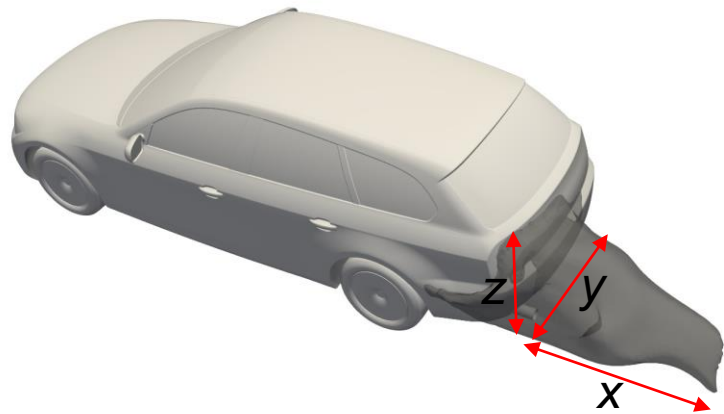


(c) Normalized cut plane integral of time-averaged pollutant mass fraction in the xy -planes.

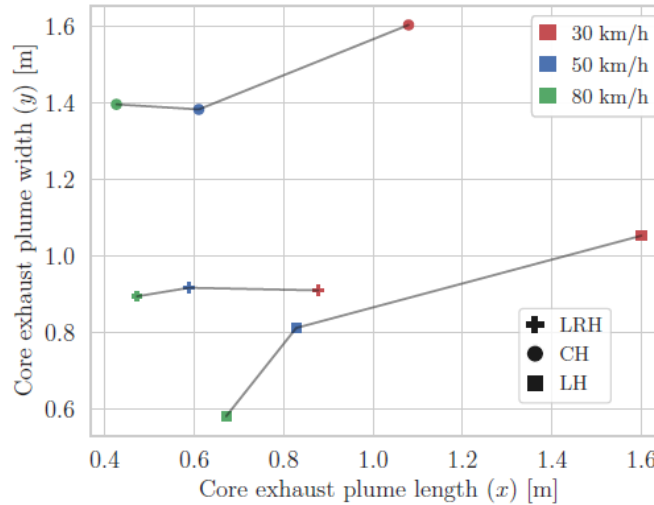
Pollutant dispersion behavior of a vehicle at 30,50 and 80 km/h.



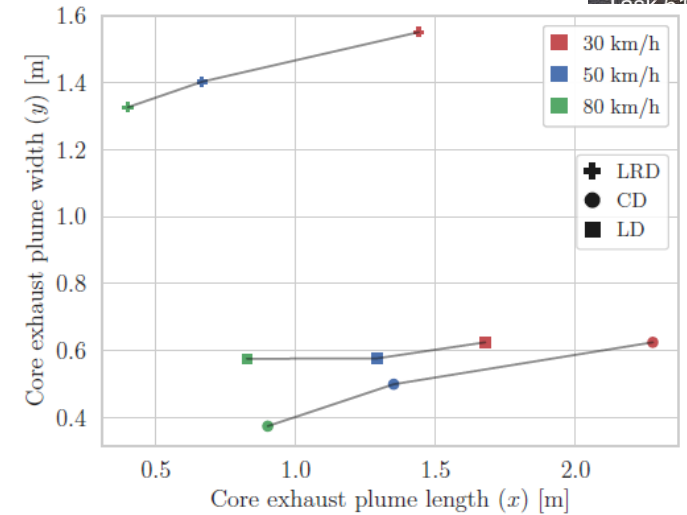
With increasing vehicle speed, the (Core) Exhaust Plume (CEP) gets shorter



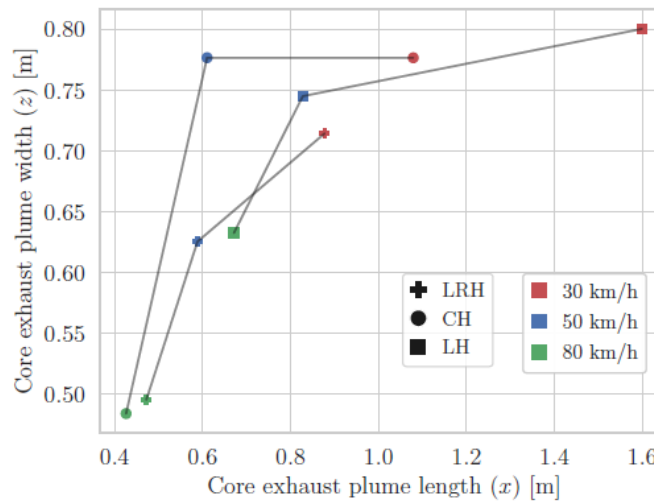
CEP is the plume up to a hundredfold dilution of the initial exhaust tailpipe concentration



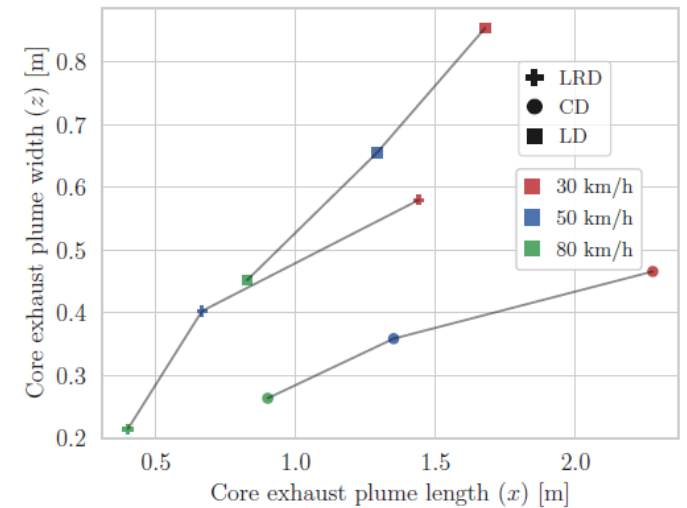
(a) CEP of horizontal tailpipes in x- and y-direction.



(b) CEP of downward oriented pipes in x- and y-direction.

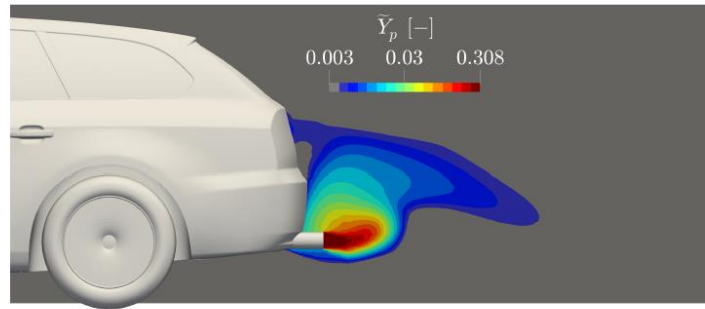


(c) CEP of horizontal tailpipes in x- and z-direction.

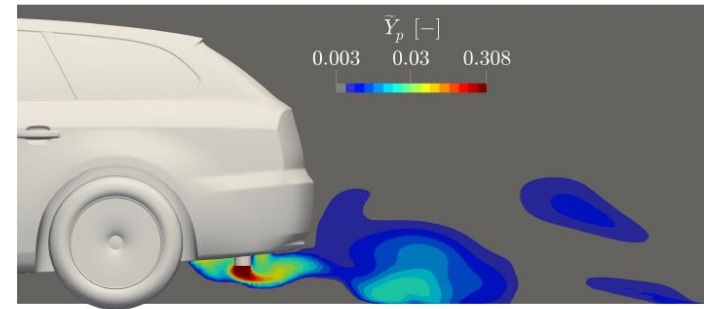


(d) CEP of downward oriented pipes in x- and z-direction.

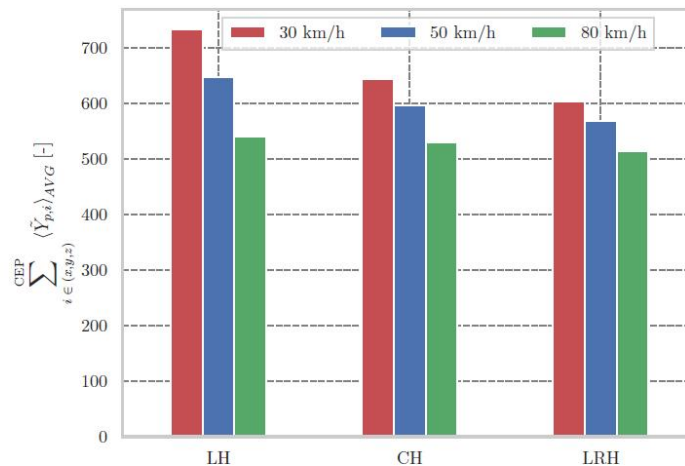
Different pipe positions change the amount of pollutant in core exhaust plume



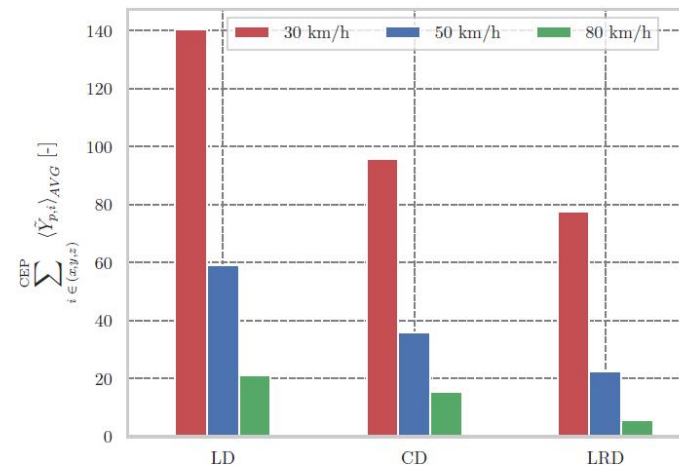
(a) xz-plane at $y = -0.56$ m-plane (LH tailpipe position).



(b) xz-plane at $y = -0.56$ m-plane (LD tailpipe height).



(c) Tailpipe locations are LH, CH and LRH.

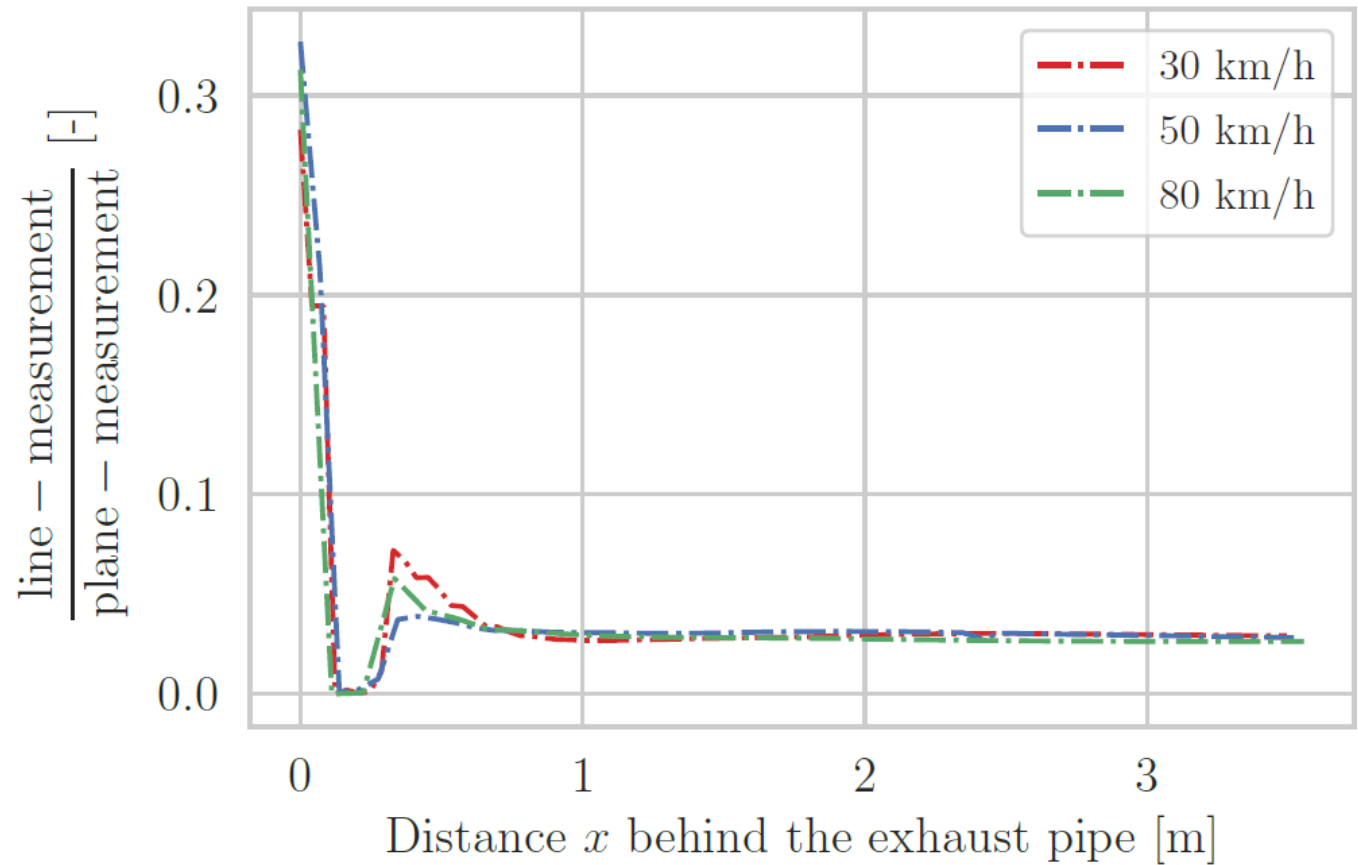
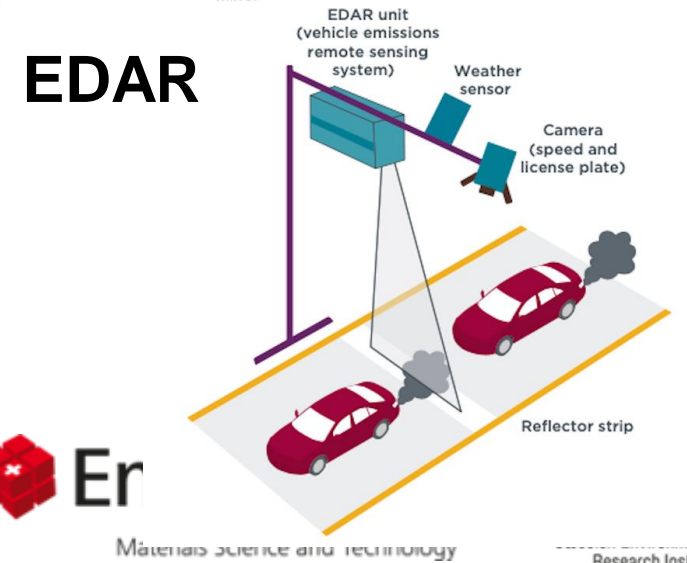
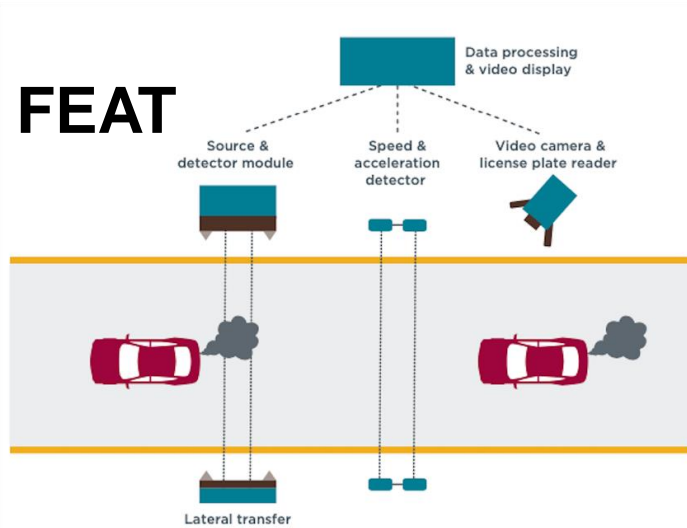


(d) Tailpipe locations are LD, CD and LRD.

Sum of all time-averaged pollutant at x, y and z in the core exhaust plume (CEP) in case of 30, 50 and 80 km/h vehicle speed. Tailpipe locations are left horizontally oriented (LH), central horizontally oriented (CH) as well as left and right horizontally oriented (LRH).

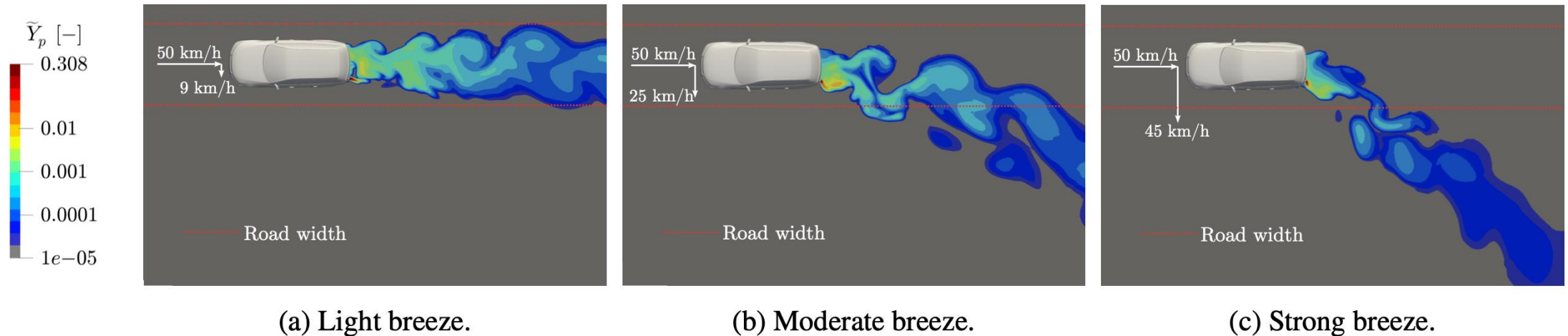


The light beam instrument can capture max. 30% of the plume captured by a laser sheet instrument



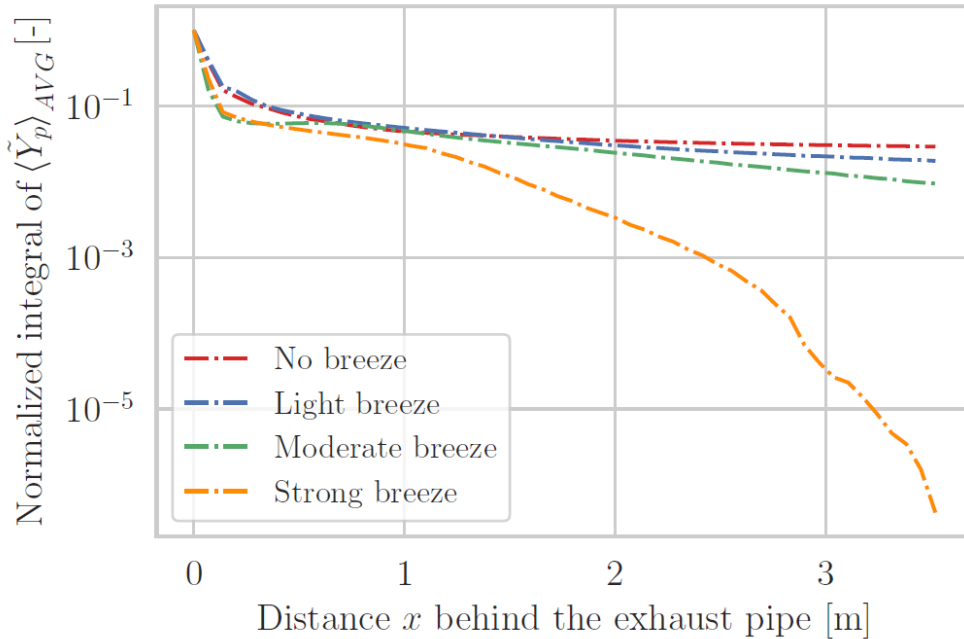
Ratio of the sum of time-averaged pollutant mass fraction of FEAT (line in y -direction at tailpipe height $z = 0.3$ m) and EDAR (yz -plane).

Increasing crosswind speed causes stronger deflection and oscillations of the exhaust plume

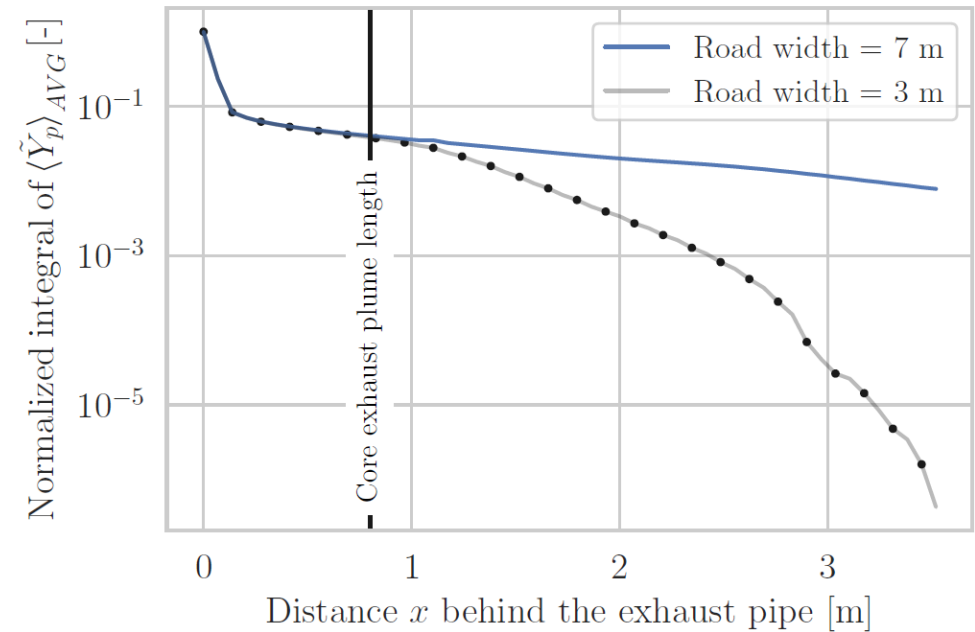


Exhaust plume deflection under influence of light, moderate and strong breeze from the right side (90°) in case of a vehicle driven at 50 km/h with a horizontally oriented tailpipe on the left. Planes are extracted for a road width of 3 m.

Core exhaust plume deflection is rather small

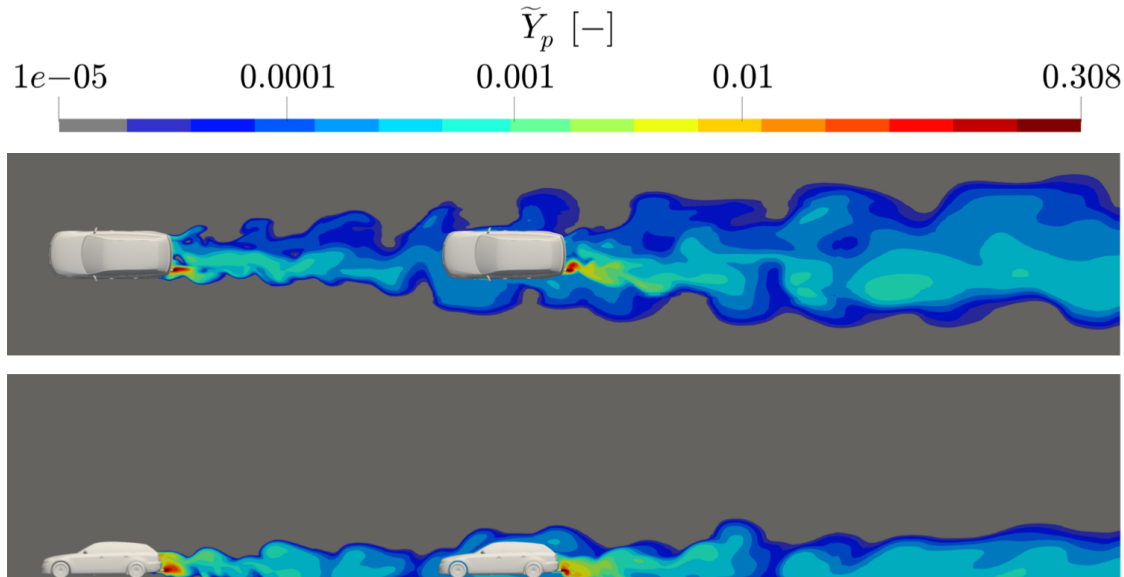


Integral of time-averaged pollutant mass fraction in yz -plane under influence of light, moderate and strong breeze coming from the right side (90°). The vehicle is driving at 50 km/h and has a horizontally oriented tailpipe on the left. Road width is 3 m.

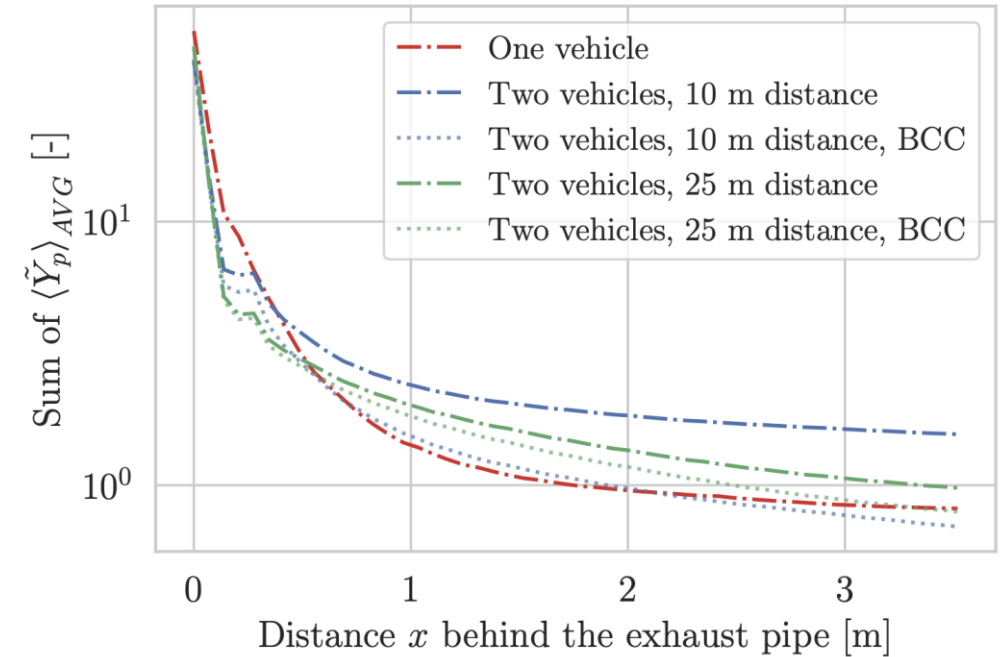


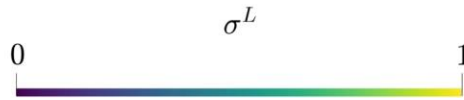
Influence of road width in case of a vehicle driving at 50 km/h with a horizontally oriented tailpipe on the left side, where crosswind is acting from the side (90°) at 45 km/h.

Vehicle ahead causes more chaotic flow in front of the following vehicle. “Background” concentration from vehicle ahead (after 10 and 25 m) is negligible



Pollutant mass fraction at $z = 0.3$ m plane (top) and $y = -0.57$ m plane (bottom) of two vehicles driving at 50 km/h 10 m apart from the other, both with horizontally oriented pipes on the left side.





Drift term:

$$Q_{u,i}^R = \begin{cases} \frac{\langle \bar{u}_i \rangle^{AVG} - \langle u_i \rangle}{\gamma_r} & \text{in LES regions and} \\ 0 & \text{in RANS regions.} \end{cases}$$

Drift term:

$$Q_{u,i}^L = \begin{cases} Q_i^{L,u} + Q_i^{L,g} & \text{in RANS regions and} \\ 0 & \text{in LES regions,} \end{cases}$$

RANS:

$$\begin{aligned} \frac{\partial \langle \rho \rangle \hat{u}_i}{\partial t} + \frac{\partial \langle \rho \rangle \hat{u}_i \hat{u}_j}{\partial x_j} &= - \frac{\partial \langle p \rangle}{\partial x_i} \\ &+ \frac{\partial}{\partial x_j} 2 \langle \rho \rangle \left[(\nu + \nu_t) \hat{S}_{ij} - \frac{1}{3} \delta_{ij} \left(\nu \frac{\partial \langle u_k \rangle}{\partial x_k} + k \right) \right] \\ &+ \langle \rho \rangle Q_{u,i}^R \end{aligned}$$

LES:

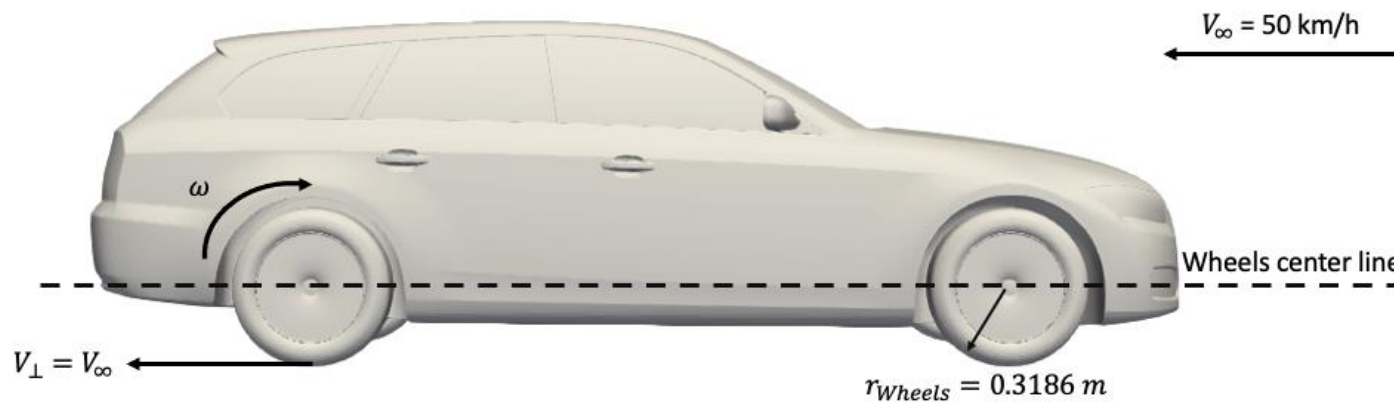
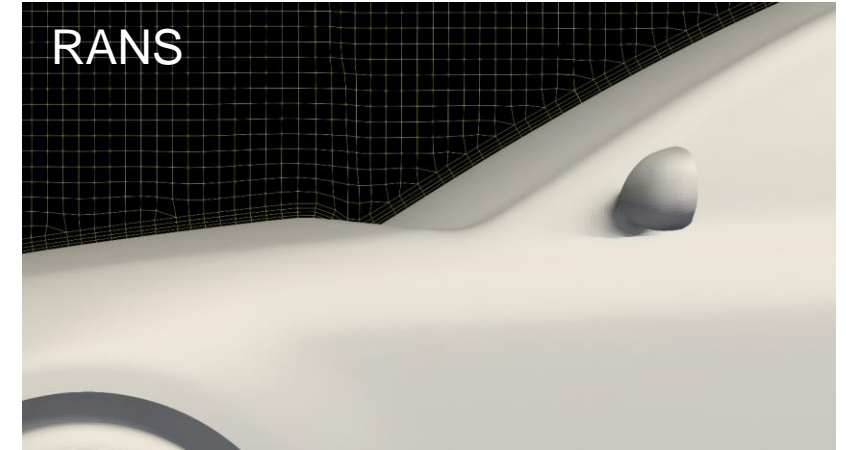
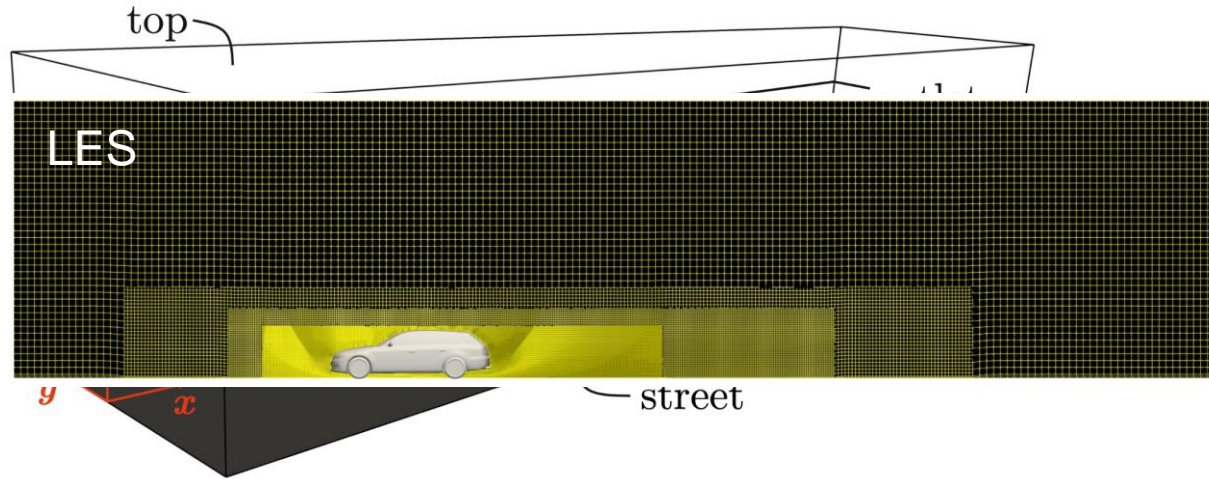
$$\begin{aligned} \frac{\partial \langle \rho \rangle \hat{u}_i}{\partial t} + \frac{\partial \langle \rho \rangle \hat{u}_i \hat{u}_j}{\partial x_j} &= - \frac{\partial \langle p \rangle}{\partial x_i} + \frac{\partial \left(\langle \tau_{ij}^v \rangle - \langle \rho \rangle \widehat{u_i' u_j'} \right)}{\partial x_j} \\ &+ \langle \rho \rangle Q_{u,i}^R \end{aligned}$$

Averaging:

$$\begin{aligned} \langle \phi \rangle^{AVG,n} &= (1 - \alpha) \phi^n + \alpha \langle \phi \rangle^{AVG,n-1} \\ \text{with } \alpha &= \frac{1}{1 + \Delta t / T} \end{aligned}$$

Consistency:

$$\begin{aligned} \langle \bar{u}_i \rangle^{AVG} &\approx \langle u_i \rangle \\ \langle \tau_{ij} \rangle^{AVG} &\approx \langle u_i' u_j' \rangle \\ \langle \varepsilon \rangle^{AVG} &\approx \varepsilon^R \end{aligned}$$



Car model: DrivAer

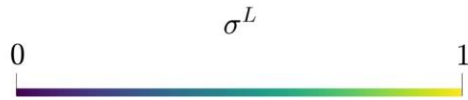
Mesh:

RANS: 2,031,997 cells

LES: 3,393,543 cells

Software: OpenFOAM





Drift term:

$$Q_z^R = \begin{cases} \frac{\langle \tilde{Z} \rangle^{AVG} - \hat{Z}}{\gamma_{zr}} & \text{in LES regions,} \\ 0 & \text{in RANS regions,} \end{cases}$$

Drift term:

$$Q_z^L = \begin{cases} Q^{L,z} + Q^{L,\zeta} & \text{in RANS regions,} \\ 0 & \text{in LES regions,} \end{cases}$$

$$Q^{L,z} = \frac{\hat{Z} - \langle \tilde{Z} \rangle^{AVG}}{\gamma_{zl}}$$

$$Q^{L,\zeta} = \left(1 - \frac{\zeta_{sgs}^{AVG}}{\zeta^{AVG}} \right) \frac{\zeta^R - \zeta^{AVG}}{\zeta^R + \zeta^{AVG}} \frac{\tilde{Z} - \langle \tilde{Z} \rangle^{AVG}}{2\gamma_{vl}}$$

RANS:

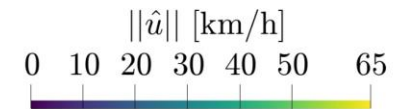
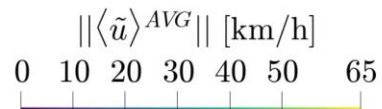
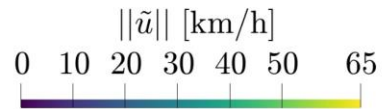
$$\frac{\partial \langle \rho \rangle \hat{Z}}{\partial t} + \frac{\partial \langle \rho \rangle \hat{u}_i \hat{Z}}{\partial x_i} = \frac{\partial}{\partial x_i} \left[\langle \rho \rangle (\Gamma + \Gamma_t) \frac{\partial \hat{Z}}{\partial x_i} \right] + \langle \rho \rangle Q_z^R$$

LES:

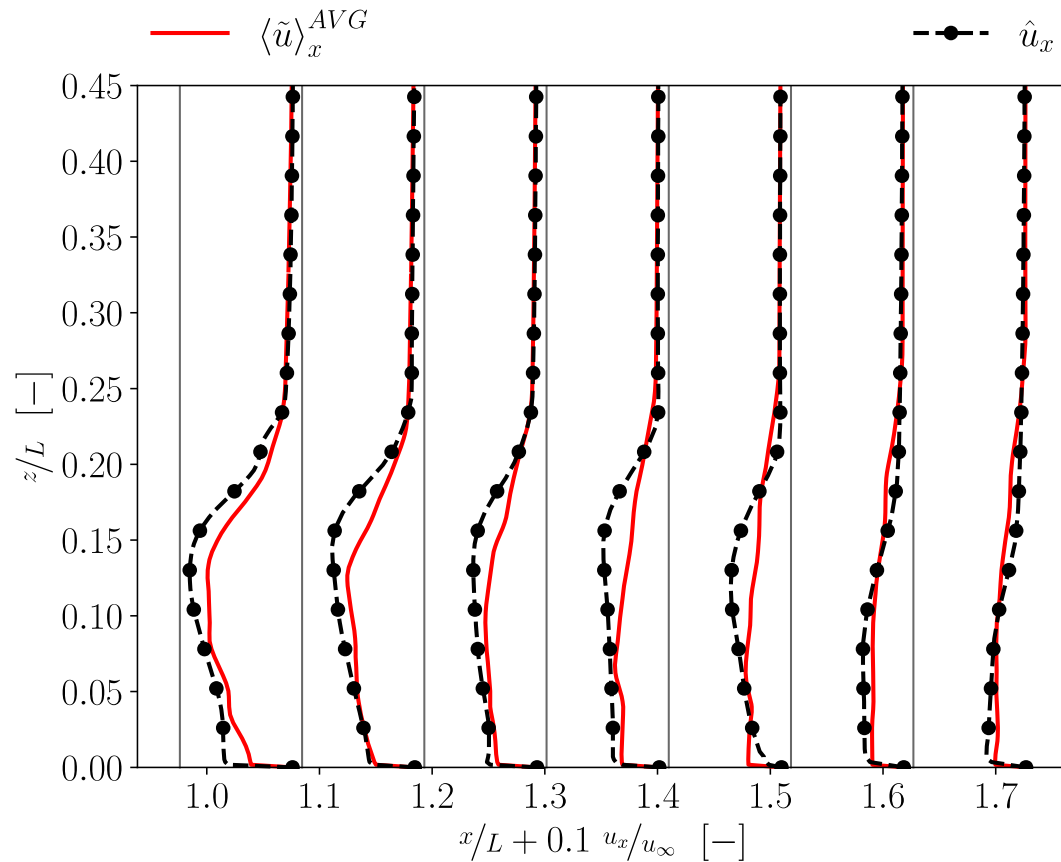
$$\frac{\partial \bar{\rho} \tilde{Z}}{\partial t} + \frac{\partial \bar{\rho} \tilde{u}_i \tilde{Z}}{\partial x_i} = \frac{\partial}{\partial x_i} \left[\bar{\rho} (\Gamma + \Gamma_{sgs}) \frac{\partial \tilde{Z}}{\partial x_i} \right] + \bar{\rho} Q_z^L$$

The averaged LES fields should be close to the URANS fields: Flow velocities

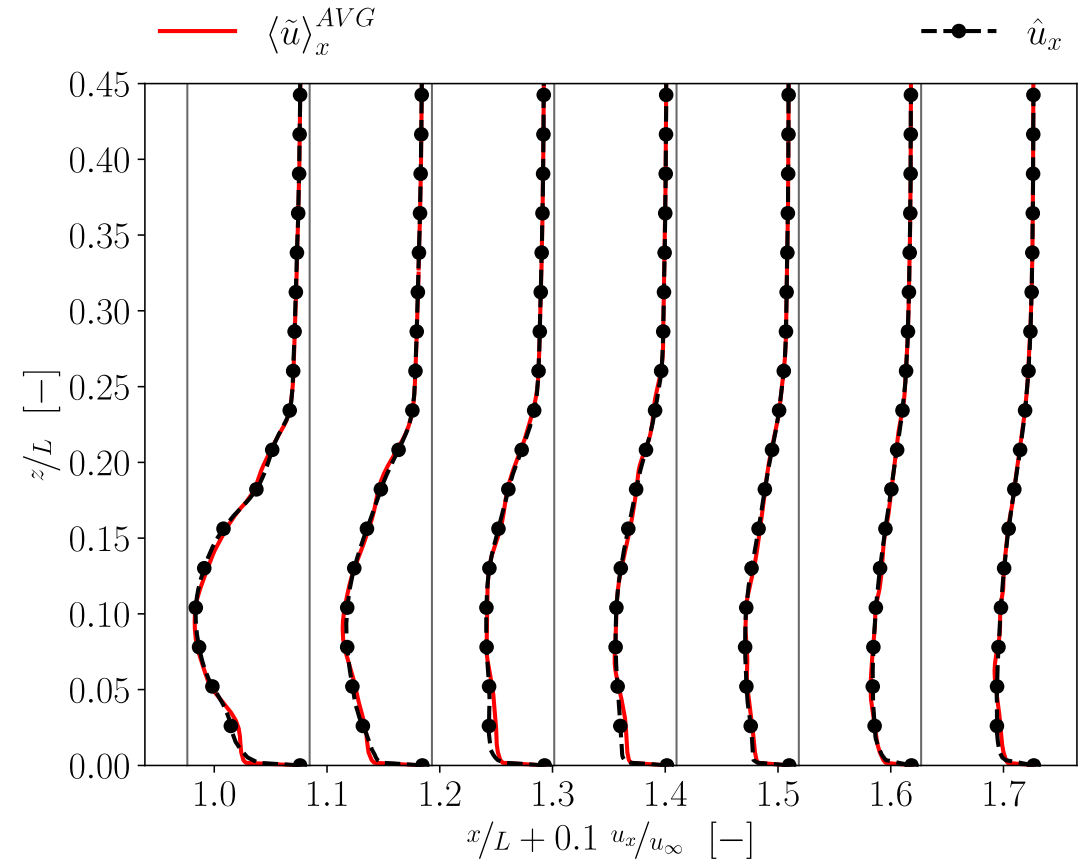
- LES provides an unsteady velocity field with fluctuations
- URANS provides an unsteady but mean velocity field without fluctuations
- Consistency is achieved between averaged LES and URANS velocities



Consistency of velocity fields

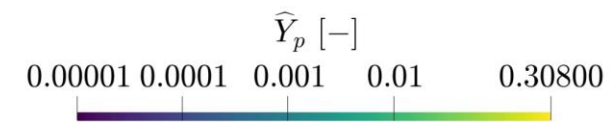
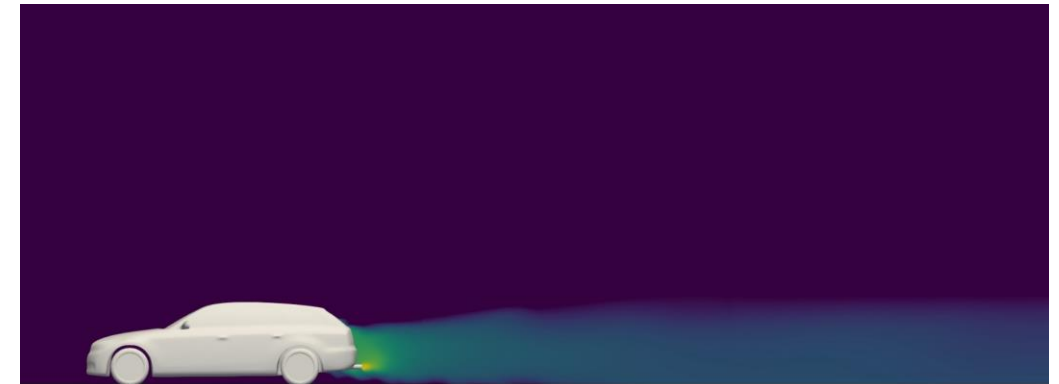
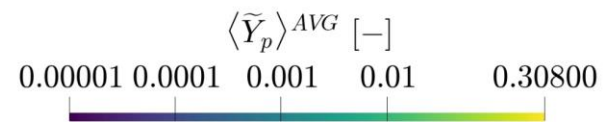
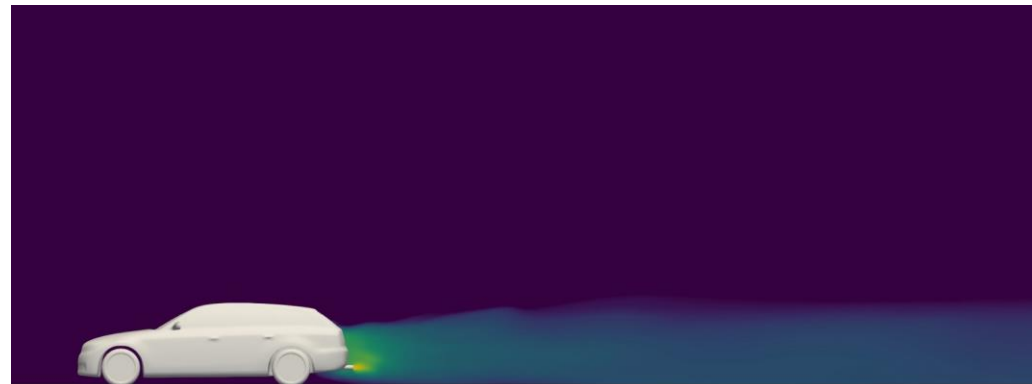
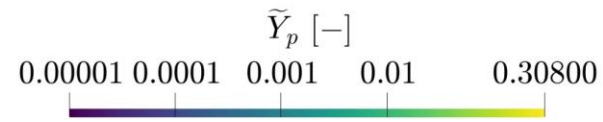
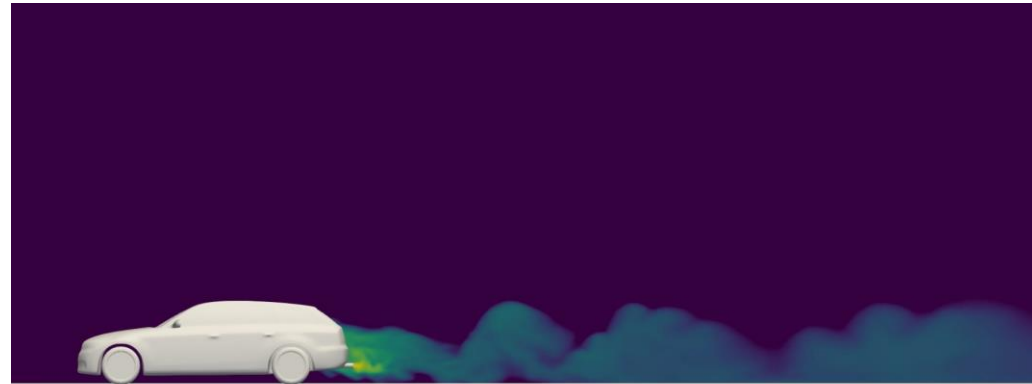


Before coupling (standalone simulations)



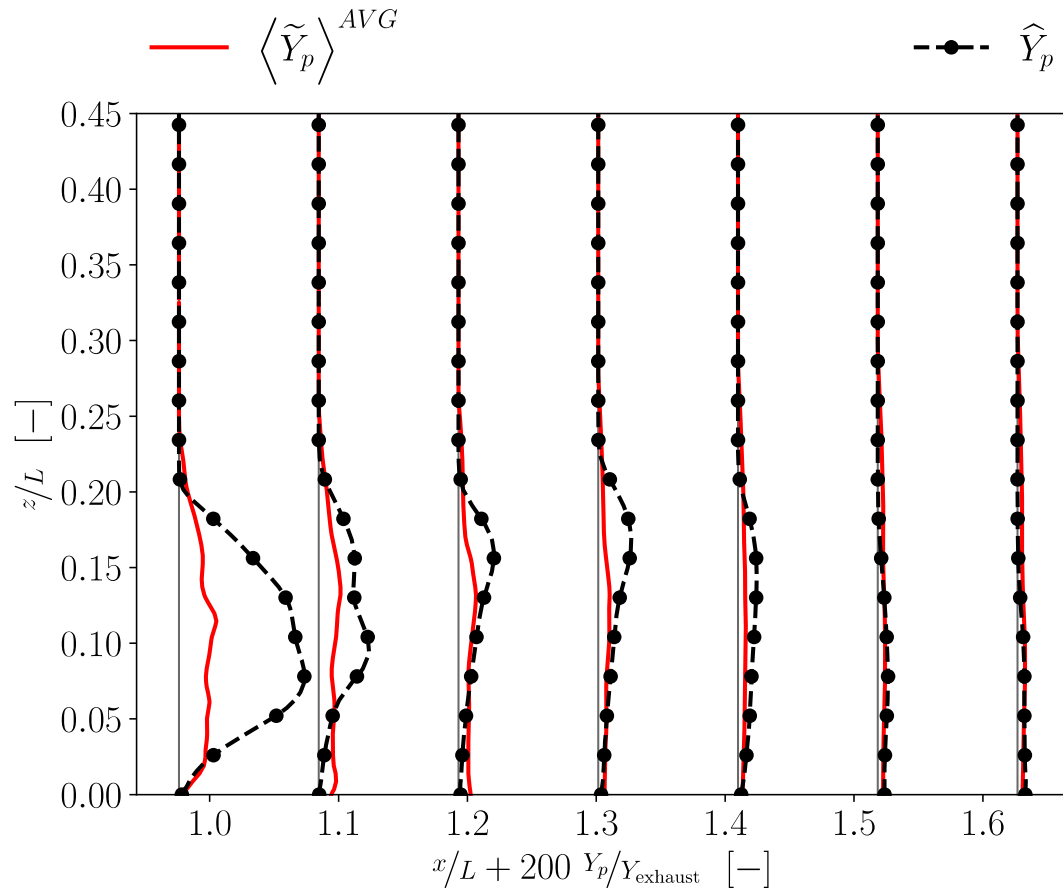
After coupling (hybrid simulation)

Consistency of pollutant concentration fields

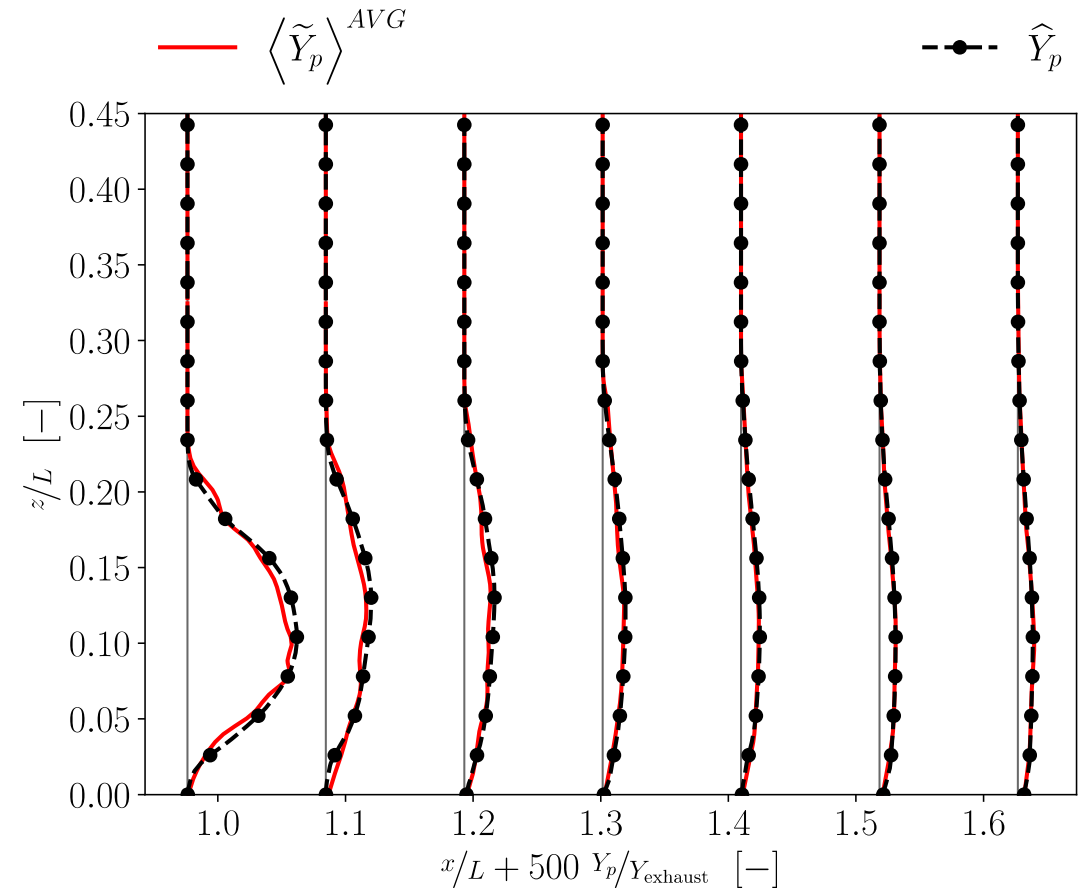


- Analogous to velocity
- Consistency is achieved between averaged LES and URANS pollutant concentrations

Consistency of pollutant concentration fields



Before coupling (standalone simulations)



After coupling (hybrid simulation)

URANS simulations of vehicle exhaust plumes with insight on remote emission sensing



Development of a consistent dual-mesh framework for hybrid LES/RANS simulations



Hybrid LES/RANS simulations of vehicle exhaust plumes
Implications for remote emission sensing



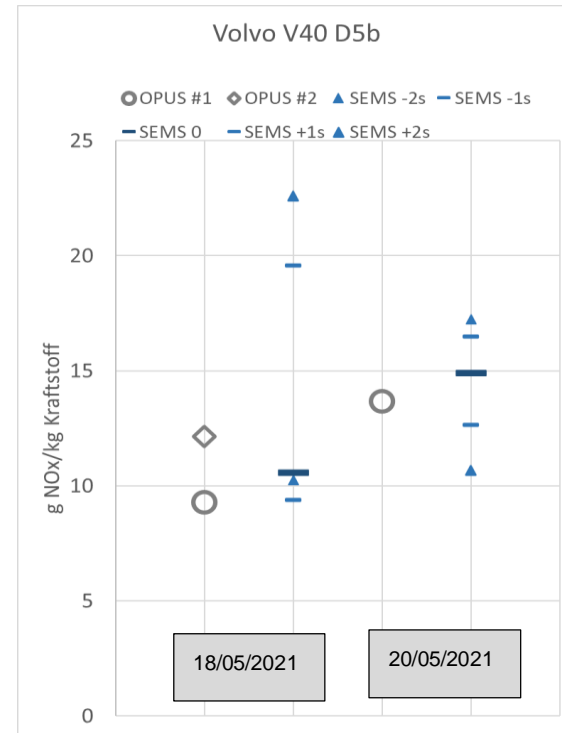
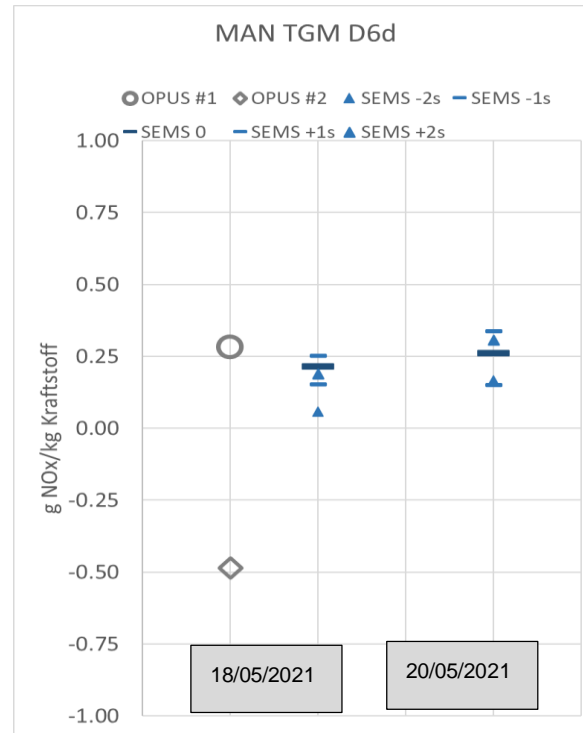
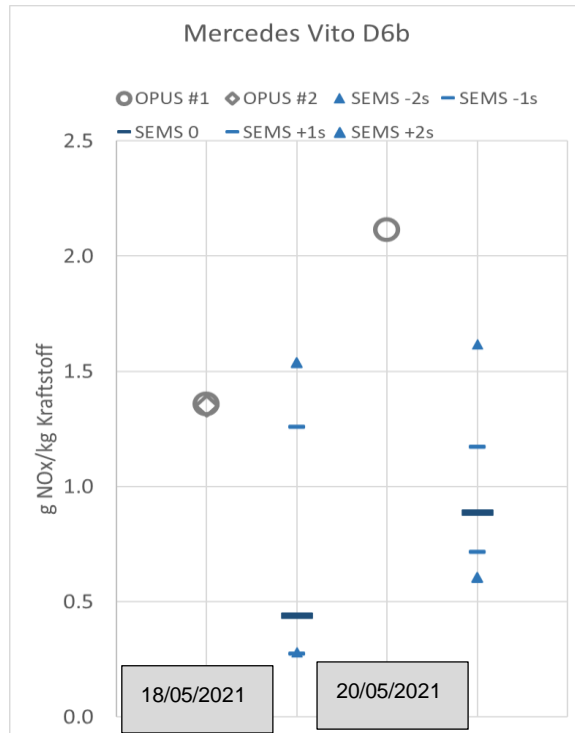
Sparse data assimilation for the optimization of unsteady flow problems

Focus: Simulations and specific evaluations of measurement data

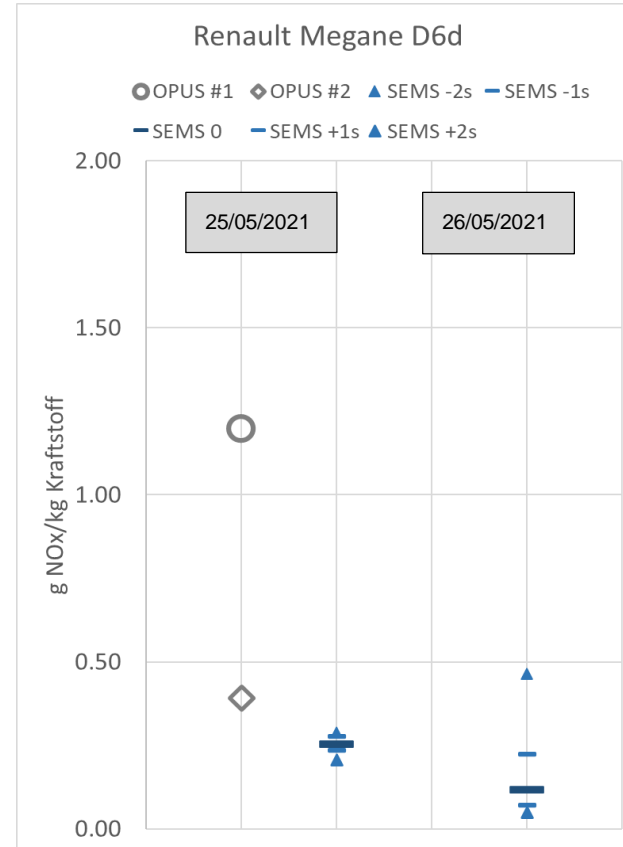
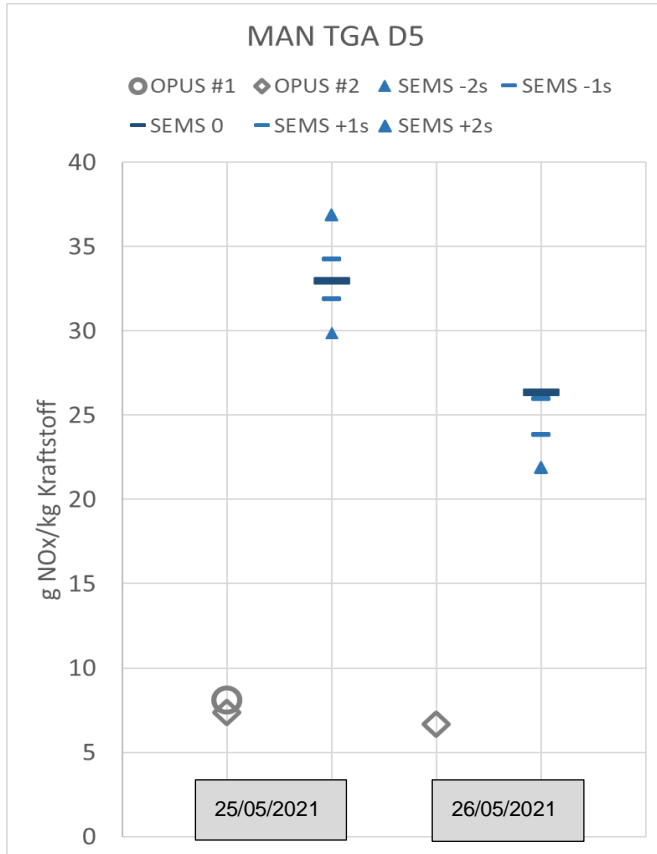


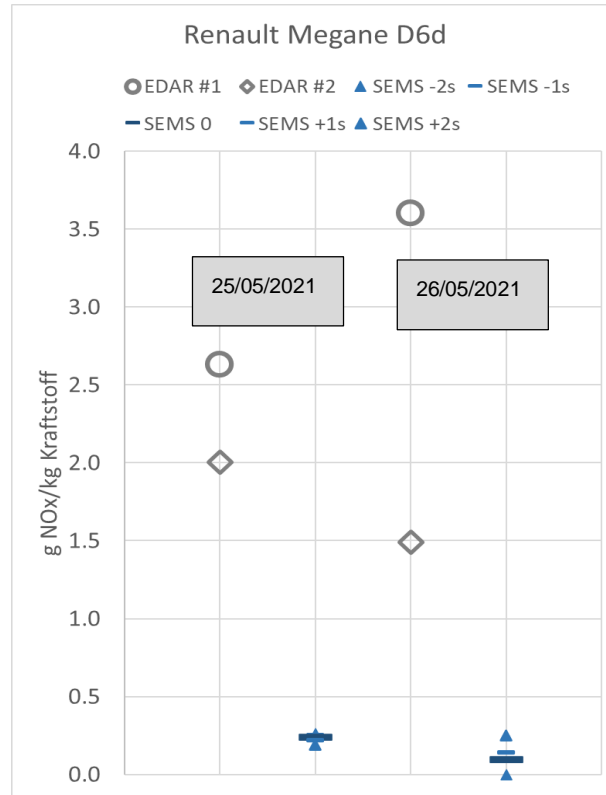
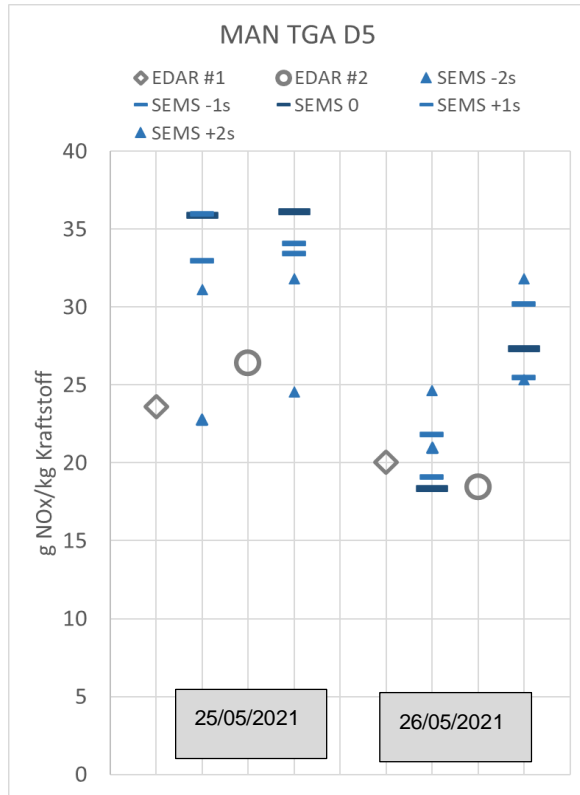
- WP 1: Numerical Simulation of the dispersion of a pollutant in the vehicle
- WP2: **Relation of RES measured data to the actual vehicle emission**
- WP 3: Potential of RES measurements for determining aging of vehicles' exhaust aftertreatment systems in the field
- WP 4: Technical exchange with the other countries in the project, other projects. Integration of the Swiss measurements in the CONOx database

Comparison of RES to vehicle on board/portable emission measurements (SEMS)



High discrepancies for low emitting vehicles (according to Euro 6)



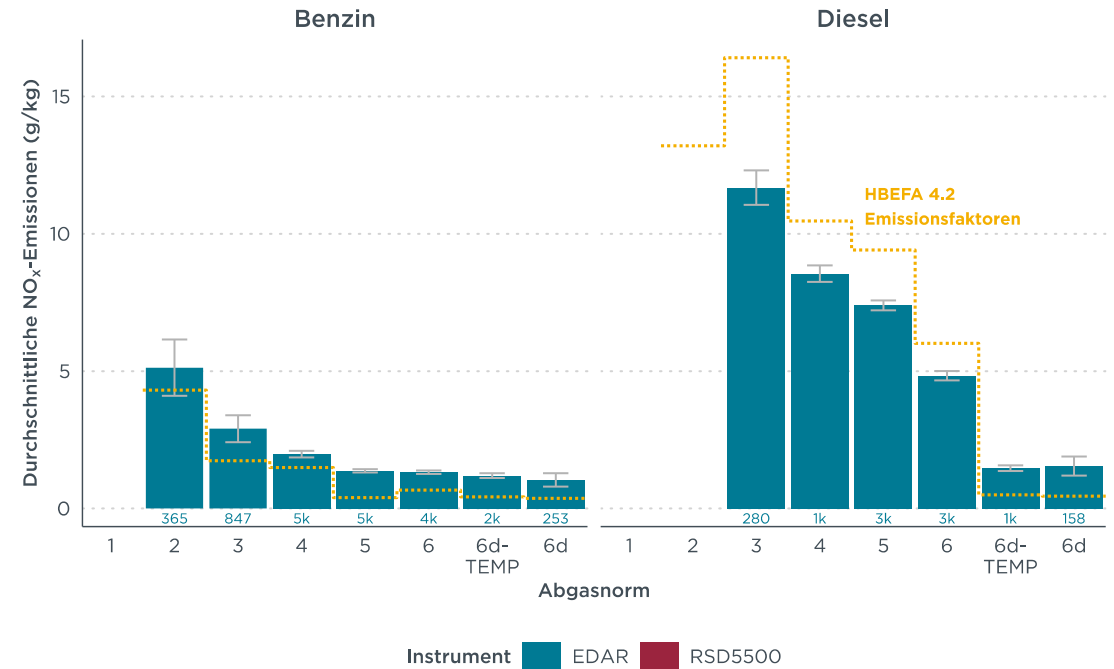
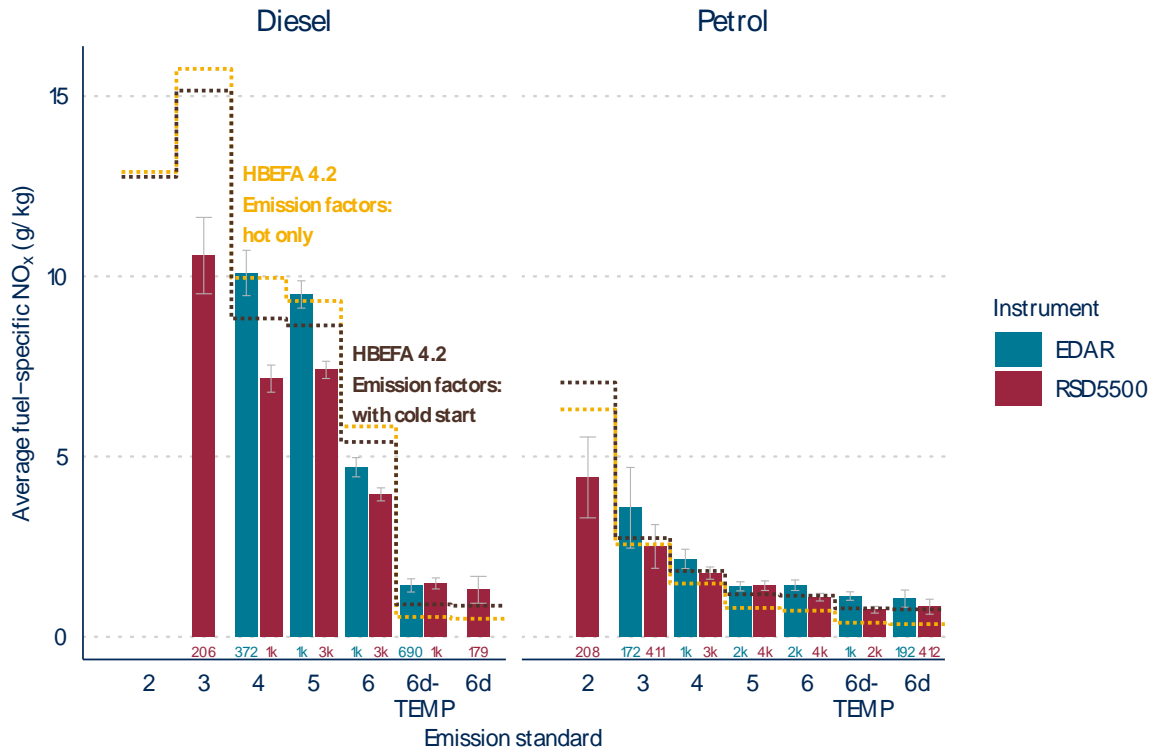


Focus: Simulations and specific evaluations of measurement data



- WP 1: Numerical Simulation of the dispersion of a pollutant in the vehicle
- WP2: Relation of RES measured data to the actual vehicle emission
- WP 3: Potential of RES measurements for determining aging of vehicles' exhaust aftertreatment systems in the field
- WP 4: **Technical exchange with the other countries in the project, other projects. Integration of the Swiss measurements in the CONOx database**

Measured values by RES near to the HBEFA 4.2 emission factors



Simulations show clearly, that the emission information is in the first 1-3m in the vehicle wake (of light duty vehicle)



- Pollutant concentrations in the core exhaust plume are only weakly affected by vehicle movement and/or environmental parameters.
- Careful application of the RES has the potential of characterizing accurately the vehicle emissions.
- While this is clear for light duty vehicles, serious doubts can be addressed towards heavy duty vehicles given the relative large distance between the exhaust pipe exit and the vehicle end.
- The accuracy of chasing measurements is also under scrutiny.
- Calibration and use of RES is rather for a specialized group of technicians.
- Quantification of the emission of very low emitting vehicles by RES is inaccurate.
- Measurement of NO₂ is imprecise.